

Atmospheric Heterogeneous Reactions of Benzo(a)pyrene

By M. Cazaunau^{1,2}, K. Le Ménach^{1,2}, H. Budzinski^{1,2}, and E. Villenave^{1,2,*}

¹ Université de Bordeaux, Institut des Sciences Moléculaires, Laboratoire de Physico-Toxicologie Chimie de l'Environnement, 33405 Talence cedex, France

² CNRS, UMR 5255, 33405 Talence cedex, France

Dedicated to Prof. Dr. Reinhard Zellner on the occasion of his 65th birthday

(Received January 16, 2010; accepted March 29, 2010)

PAH / Reactivity / Benzo(a)pyrene / Nitrobenzo(a)pyrene / Ozone / Nitrogen Dioxide / Hydroxyl Radical / Atmospheric Particle / Silica / GC-MS

This experimental study deals with heterogeneous reactions of benzo(a)pyrene (BaP) with ozone, nitrogen dioxide and hydroxyl radicals. BaP was adsorbed on silica particles chosen here as a model of mineral atmospheric particles. Compound extractions were assisted by focused microwave and analyses were performed by gas chromatography coupled with mass spectroscopy in single ion monitoring mode. Pseudo-first order rate constants were obtained from the fit of experimental decays of particulate-BaP concentration versus reaction time. Second order rate constants were determined considering the different oxidant gaseous concentrations except for the case of hydroxyl radicals where only a pseudo-first order rate constant was proposed. Values obtained at room temperature are $(2.1 \pm 0.5) \times 10^{-15} \text{ cm}^3 \text{ molecule}^{-1} \text{ s}^{-1}$ for (BaP + ozone), $(5.8 \pm 1.4) \times 10^{-16} \text{ cm}^3 \text{ molecule}^{-1} \text{ s}^{-1}$ for (BaP + nitrogen dioxide) and $(3.4 \pm 0.8) \times 10^{-2} \text{ s}^{-1}$ for (BaP + OH) reactions. Products have only been investigated for the NO₂ and the OH (in the presence of NO_x) reactions. 1-, 3- and 6-nitrobenzo(a)pyrenes were detected as degradation products and quantified. Reaction rate constants for product formation are $(3.7 \pm 0.9) \times 10^{-16} \text{ cm}^3 \text{ molecule}^{-1} \text{ s}^{-1}$ for 6-NBaP, $(2.2 \pm 0.6) \times 10^{-17} \text{ cm}^3 \text{ molecule}^{-1} \text{ s}^{-1}$ for 1-NBaP and $(5.3 \pm 1.3) \times 10^{-17} \text{ cm}^3 \text{ molecule}^{-1} \text{ s}^{-1}$ for 3-NBaP. 1-, 3- and 6-nitroBaP account respectively for approximately 5%, 12% and 83% of total nitrated species. If in the presence of only nitrogen dioxide, BaP was totally degraded within few minutes, only 20 to 25 % of the initial BaP led to nitrated compounds when reacting with OH (in the presence of NO_x).

1. Introduction

Polycyclic Aromatic Hydrocarbons (PAHs) are ubiquitous contaminants in the environment. Such compounds are mainly formed during natural and anthropo-

* Corresponding author. E-mail: e.villenave@ism.u-bordeaux1.fr

genic incomplete combustion processes [26]. In the atmosphere, almost 90% of PAH sources are anthropogenic (Finlayson-Pitts *et al.*, 1986). They are well-known to have mutagenic and/or carcinogenic activities for humans through metabolic activation pathways [12]. In 1979, US-EPA defined 16 PAHs as priority pollutants [33] with a particular focus on benzo(a)pyrene (BaP) which is one of the most mutagenic and carcinogenic PAH [13, 28]. BaP is nowadays used by regulators as the basis for quantitative risk estimation of PAH-containing combustion by-products [62].

In the atmosphere, due to its low vapour pressure and its high molecular weight, BaP is mainly present adsorbed onto particulate matter [19] and may be adsorbed either on carbonaceous particles, directly emitted from combustion processes [1, 44, 59], or on mineral particles arising from soil erosion [54].

After formation and emission, particulate-BaP may be subject to various degradation processes such as photodegradation and chemical oxidation with O_3 , NO_x or OH. These reactions are important to consider as they can lead to the formation of particularly toxic products like oxygenated and/or nitrated compounds. It has already been demonstrated that such species are generally much more toxic than the BaP itself [30].

Although considerable research has already been performed on the degradation of BaP under simulated atmospheric conditions [1, 5, 6, 16, 18, 44, 56, 57, 59], there is still a lack of knowledge about the kinetics and fate of PAHs adsorbed on particles. Several studies have been performed on different types of particulate matters such as natural carbonaceous particles [18, 36, 49], artificial carbonaceous particles [17, 42, 44, 49, 59, 60], model or natural mineral particles [5, 6, 25, 50, 52, 56, 57, 66] and salt aerosol [41]. These studies exposed coated-particles to different gaseous species using various experimental set-ups (reaction chamber, fast flow and quasi-static reactors...) in order to measure the kinetics of oxidation reactions of adsorbed compounds and identify or predict their degradation products. For the reaction of BaP with ozone, oxygenated compounds, such as ketones, quinones, lactones and carboxylic acids, predominate as degradation products [30, 65]. When looking at potential oxygenated particulate products in the atmosphere, it may be noted that benzo(a)pyrene dione has for instance been detected in natural particulate samples in different countries in the world [7, 36]. In laboratory studies, experiments have demonstrated the formation of BaP-6, 12-dione, BaP-1, 6-dione and BaP-3, 6-dione when artificial soot was exposed to ozone [37]. Lactones can be formed both by photoreaction and/or ozonolysis and contribute to a high mutagenicity of particulate matter [30]. Reactions with hydroxyl radicals in the presence of nitrogen dioxide can also lead to the formation of oxygenated compounds such as hydroxylated BaP, formed by the loss of one molecule of nitrous acid [16, 61]. Nitrated compounds have also been found on ambient particles [2, 3, 4]. The origin of the formation of nitro-PAHs may vary: they may be formed directly during combustion processes or in the gas phase during the atmospheric transport or by heterogeneous reactions in the atmosphere at the gas/particle interface. During such heterogene-

ous processes, BaP may react with the nitrate radical or nitrogen dioxide by electrophilic substitution with elimination of nitrous acid [7, 21, 34, 35]. The formation of nitrated species may also be initiated by the hydroxyl radical, followed by reaction with nitrogen dioxide and the loss of one molecule of water [9, 15, 20, 61]. Nitro-BaP and dinitro-BaP are only occasionally selected for chemical analysis despite the fact they are strong direct-acting mutagens [27, 30, 46, 47]. For instance, 6-nitro-BaP has already been detected on atmospheric particles [2, 3, 4]. In laboratory studies, 1- and 3-nitro-BaP [38] and dinitroBaP [30] have been detected to be generated by similar processes.

In this work, heterogeneous reactions of O₃, NO₂ and OH (in the presence of NO_x) with BaP adsorbed on silica particles have been investigated. Silica was chosen as a model of atmospheric particles: first it belongs to the major elements as oxides in the continental crust [63] and it is also one of the most used inorganic proxy in heterogeneous reaction studies due to its well-known physico-chemical properties [5, 6, 10, 50, 56, 57, 66]. Room temperature second order reaction rate constants have been determined for the reactions with O₃ and NO₂ and compared to previous measurements. Finally, identification and quantification of some resulting degradation products were performed.

2. Experimental

2.1 Chemicals

The chemicals used in this work were as follows: Benzo(a)pyrene ($\geq 97\%$, Aldrich), 6-nitro-benzo(a)pyrene (99.8 %, Promochem), benzo(a)pyrene d12 (98 %, Cambridge Isotope Laboratories), benzo(b)fluoranthene d12 (98 %, Cambridge Isotope Laboratories). Analytical grade solvents were dichloromethane (Acros Organics, for residue and pesticides analysis) and isooctane (Scharlau, HPLC Grade). Standard solutions were prepared by dissolving standard crystals in isooctane. Standard and solvent quantities were measured by gravimetry. These solutions were kept at -20°C and in complete darkness.

2.2 Silica particles

Silica particles IT70–5 were supplied by Interchim. According to their certificate of analysis, the silica particles have an average particle diameter of 5 μm and an average pore diameter of 70 Å. The diameter of these particles is situated in the coarse particle mode. These particles have well-defined properties already detailed in a previous work [56]. Their specific surface area is about 500 $\text{m}^2 \text{g}^{-1}$. If this value is higher than those reported for natural mineral particles (Saharan sand and Gobi dust BET surface areas are typically around 5 and 10 $\text{m}^2 \text{g}^{-1}$ respectively [64]), it allows us to compare this work with previous reported data, particularly by our group, on heterogeneous reactions of PAHs adsorbed on different types of particles [17, 18, 57].

2.3 Particle preparation and storage

The particles were first cleaned by ultrasonication (3 times) in dichloromethane (Acros Organics, for residue and pesticides analysis) and allowed to dry at room temperature. Benzo(a)pyrene was individually coated on silica particles using liquid–solid adsorption. The coating procedure has already been described in a previous work [51, 57]. Particulate BaP concentrations were always about $500 \mu\text{g g}^{-1}$. The surface coverage was calculated, to be lower than 1 % of a monomolecular layer. Note that this does not exclude a partial formation of multilayers of PAHs on the surface.

In order to prevent any photodegradation processes, already observed in the case of silica particles [10], all the prepared particles were stored at room temperature, in the dark and in amber glass flasks.

2.4 Benzo(a)pyrene

2.4.1. Quantification

Particulate BaP concentration measurements were performed using internal standard quantification and furthermore, internal standard was quantified by a syringe standard. Such double quantification allowed the calculation of internal standard recovery yields and hence to check that internal standard, and therefore native BaP, was not lost during the analytical procedure. Perdeuterated benzo(a)pyrene and benzo(b)fluoranthene were respectively used as internal and syringe standards and were supplied by Cambridge Isotope Laboratories. Quantifications were performed using a calibration solution, prepared with native BaP and perdeuterated standards (BaP d12 and BbF d12). This solution, injected before, between and after each analysis, allowed us to calculate the BaP and the standard response factors and therefore to check and monitor the conditions of the chromatographic and detection systems.

2.4.2 Analytical procedure

After the reaction (and before the extraction), the samples and the internal standard were introduced in a “matras” (a pyrex test tube by Prolabo), the internal standard quantity being controlled by gravimetry. BaP was extracted using focused microwave assisted extraction (Microdigest 301, Prolabo) in 45 mL of dichloromethane at 30W during 15 min. The complete extraction procedure was validated and detailed previously [43]. The extracts were filtered on glasscoton (VWR) previously cleaned by three successive ultrasonications in dichloromethane. Dichloromethane was evaporated and change in iso-octane (2,2,4-trimethyl pentane, HPLC grade, Scharlau) using a vacuum evaporation system (Rapidvap, Labconco), which uses vortex motion, vacuum and heat (70%, 900 mbars and 50°C during 30 min). Finally, syringe standard was added to the samples just before the GC-MS analysis.

2.4.3 GC-MS analysis

Sample analyses were performed by gas chromatography coupled to mass spectrometry (GC-MS), using a system coupling an HP model series 6890 Gas Chromatograph with an HP model 5973 selective detector (Agilent Technologies). The column was a 30m×0.25mm i.d.×0.25 μm film thickness (HP 5MS, Hewlett Packard). 1 μL of each sample was introduced via splitless mode injection. The PTV injector temperature was 270°C, and the oven temperature was held at 70 °C for 2 min, then programmed from 70 to 300°C at a rate of 10°C min⁻¹ and held at 300°C for 10 min. Helium (He 99.9999+% purity, Linde Gas) was used as carrier gas at a constant flow of 1 mL min⁻¹. The interface temperature was kept at 290°C for analysis. Ionisation was achieved by electron impact (70 eV) and mass detection was performed in selected ion monitoring mode. The ion molecular masses were chosen to detect BaP and perdeuterated standards.

2.5 Reaction systems

2.5.1 Description of experimental set-ups

All experimental set ups used in this work have already been described in details elsewhere [15, 17, 18, 45, 48, 51, 56, 57]. Only the main features are described below for each oxidant:

Ozone

The ozonolysis set-up consists of a quasi-static reaction cell where the particulate-BaP, previously deposited on a quartz fiber filter, is placed during different ozone exposure time. Ozone is generated using a low pressure mercury lamp, photolysing an Oxygen (99.999+% purity, Linde Gas)/Nitrogen (99.999+% purity, Linde Gas) mixture. The ozone concentration is finally measured using a home-made UV spectrophotometer. With this set-up, ozone concentration may typically vary from 7×10^{12} to 2.4×10^{13} molecule cm⁻³. Note that in order to avoid any interference due to the ambient light, ozone reaction has been investigated in a total darkness.

Nitrogen Dioxide

The BaP-coated silica particles are placed using a filter in a fast flow reactor (2.4 cm inside diameter/48 cm long Pyrex tube). A mixture of nitrogen dioxide (5% NO₂ in Helium 99.995% purity, Alphagaz) diluted in Helium (99.9999 % purity, Alphagaz) is introduced in the reactor via a movable injector (1 cm inside diameter, 60 cm long quartz tube) sliding into the reactor. Total pressure was held to (1.8±0.1) Torr with a total volumetric flow rate of 1 L min⁻¹. NO₂ concentration was controlled by Tylan FC2900V mass flow controller and ranged from 2.0×10^{13} to 5×10^{13} molecule cm⁻³.

Hydroxyl radical

Experiments were performed in the fast flow reactor quoted above, by monitoring the OH concentration using laser-induced fluorescence (LIF). OH radicals were generated by the fast ($\text{H} + \text{NO}_2 \rightarrow \text{OH} + \text{NO}$) reaction (Sander *et al.*, 2003). H atoms were produced by hydrogen impurities from Helium (Alphagaz 1, Air liquide) passing through a microwave discharge (Raitek LRE 300, 2450 MHz). OH radicals were directly introduced into the main reactor via the movable injector coated with halocarbon wax (Halocarbon Product) in order to prevent most of the loss of OH radicals on the walls before arriving in the reactor. NO_2 was in a large excess in order to ensure a complete stoichiometric conversion of H atoms. Total pressure was held to (1.5 ± 0.1) Torr with a total volumetric flow rate of 0.775 L min^{-1} .

OH initial radical concentration was calibrated using two different methods. The first method was consisting in slowly decreasing the NO_2 concentration until the extinction of the LIF signal, allowing to extrapolate a minimal concentration of NO_2 to generate OH radicals of $1.4 \times 10^{12} \text{ molecule cm}^{-3}$. The second method was consisting in adding well-known concentrations of H_2 (5% H_2 in Helium 99.995% purity, Air Liquide) and waiting for the LIF signal to be multiplied by a factor of 2, allowing to extrapolate a value for initial OH concentration of $1.5 \times 10^{12} \text{ molecule cm}^{-3}$. Finally, the loss of OH radicals on the filter + silica particles system alone was evaluated from the LIF signal to be around 60%, allowing to conclude to the value of $5.8 \times 10^{11} \text{ molecule cm}^{-3}$ for the initial OH radical concentration in our experiments.

Considering all the uncertainties on the calibration method detailed above, it was decided that only qualitative information will be proposed for the hydroxyl radical concentration in this work.

2.5.2 Kinetic conditions

For all oxidants, a complete degradation of particulate-bound BaP was observed after a certain exposure time. For each experiment, the kinetic information was obtained by monitoring the remaining concentration of benzo(a)pyrene versus exposure time to O_3 , OH and/or NO_2 . Specific details are provided below.

Ozone

Ozone concentration was measured all along the reaction time and no variation was observed under our experimental conditions. Gaseous O_3 residence time in the reactor (about 1 s) was negligible compared to the BaP lifetime.

Nitrogen dioxide

Assuming that all losses on the injector and reactor walls were negligible, NO_2 partial pressure before reaching the sample was equal to the value set by the mass flow controller (taking into account the dilution in Helium flow). In the

presence of water adsorbed on silica particles, NO_2 may be converted to HONO and HNO_3 [22]. However, under our experimental conditions (dried silica particles and gaseous environment), NO_2 loss on surfaces was negligible compared to the amount of NO_2 available for the reactions [50, 56].

Hydroxyl radical

OH radicals were produced upstream from the reactor. Loss on injector walls was negligible [11] but loss on filter and silica (with no BaP) was measured to be approximately equal to 60 % of the total initial OH radical produced by the microwave discharge, as already detailed above. Online OH measurement during the reaction time did not show any fluorescence variation on the detector keeping the same injector position, meaning that the OH concentration was kept stationary all along the reaction.

For each oxidant, secondary reactions implying oxidation products were first considered as negligible and finally verified a posteriori. NO radicals formed simultaneously with OH do not react with PAHs [17] and do not further interfere in the mechanism as their concentration (equal to that of OH) is always too small compared to that of NO_2 . Experiments were performed for three different concentration of oxidant (except for the hydroxyl radical) in order to verify the elementary nature of the reaction. Pseudo-first order rate constants derived from the three experimental data sets were proportional to the oxidant concentration demonstrating that the reaction of BaP with NO_2 or with O_3 was the predominant reaction and the limiting step (see part 3).

2.6 Data analysis

2.6.1 Pseudo-first order rate constant measurement

Concentrations vs. time were normalised i.e. the BaP concentration measured in $\mu\text{g g}^{-1}$ of particles after an exposure time t was divided by the corresponding initial particulate-BaP concentration (measured at $t = 0$), leading to a normalised particulate concentration of compound in %. Experimental data points were fitted by a simple mono-exponential function allowing to determine pseudo-first-order rate constants (k^{I}) for each oxidant concentration value, using non linear least square fitting. All experiments were repeated at least three times and for three different oxidant concentration values (in the case of O_3 and NO_2 only), and were very reproducible, resulting in data analyses with a high consistency. Note that all experimental data obtained (excepted in the case of OH) were finally presented on a single graph by recalculating the reaction times: concentration of oxidants (included in the pseudo-first order rate constant values) and reaction times are interchangeable in first order kinetic laws, allowing to have a maximal number of data points available to fit the results.

Similarly, experimental data points relative to the NO_2 oxidation product formation were fitted using first-order exponential growths, demonstrating that

decays corresponding to BaP reaction with NO₂ and growths describing the formation of oxidation products present the same global reaction rate (within uncertainties).

2.6.2 Second order rate constants

For gas-phase reactions, second order rate constants are often determined by dividing pseudo-first order rate constants by the reactant concentration. In most heterogeneous reactivity studies [23, 24], uptake coefficients are usually extracted from kinetic measurements, considering the fate of the oxidant vs. reaction time. In some cases, authors considered that the reactions occurred between two adsorbed species, according to a Langmuir–Hinshelwood mechanism [59]. Second-order surface reaction rate constants are therefore calculated in square centimeters per second by dividing the pseudo-first order rate constants by the concentration of ozone adsorbed on free active site on the surface. The active site surface concentrations for the silica particles used in this study being not known; such rate constants were not calculated. In other studies, [5, 32, 66], second order rate constants were calculated similarly to gas-phase reactions constants, suggesting that reactions occurred between a gaseous oxidant and a surface-bounded PAH molecule. Since values of k^I were demonstrated to be proportional to gaseous oxidant concentration under our experimental conditions (and in these concentration ranges), second order rate constants were calculated considering such gaseous oxidant concentrations [17, 18, 51, 55, 56].

2.6.3 Uncertainties determination

Errors on internal and syringe standards weighting, on silica particles weighting, on chromatographic peak integration and on GC-MS measurements were considered as random errors. Total random error was estimated by the standard deviation on the exponential coefficients obtained from the nonlinear least square fit of the experimental points, and was varying between 5% and 10%. Systematic errors (oxidant concentration, pressure, temperature, and calibration of mass flow controllers) were also taken into account. Finally, global uncertainties (random + systematic) on the second order rate constant values were evaluated to be about 25%.

3. Results and discussion

3.1 Analytical procedure validation

Analytical procedure validation was already reported by our group for different types of particles (graphite, silica, diesel exhaust and urban dust...) [43, 57]. In the present work, silica particles were doped with a solution of well-known concentration of BaP. Benzo(a)pyrene was then extracted from coated particles and analysed. Resulting recovery yields for BaP and perdeuterated BaP were

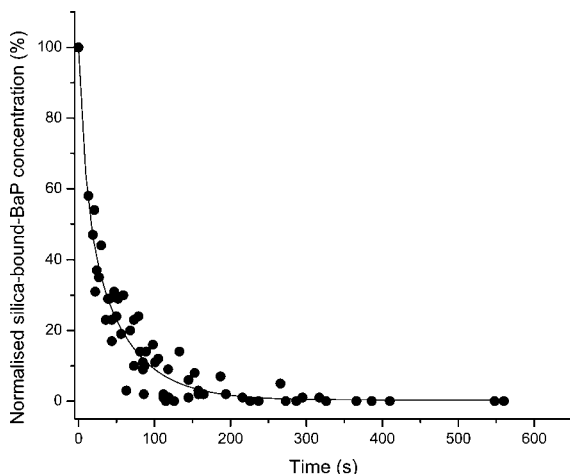


Fig. 1. Normalised concentration of BaP adsorbed on silica particles as a function of ozone exposure time, represented for $[\text{O}_3] = 1.4 \times 10^{13} \text{ molecule cm}^{-3}$.

respectively of $(96 \pm 2) \%$ ($N = 3$) and $(88 \pm 2) \%$ ($N = 3$) allowing to validate the analytical protocol.

3.2 Desorption

Prior to the study of BaP oxidation reactions, it was first necessary to verify that no potential desorption of BaP from the silica particles was occurring during the reaction time. BaP-coated-silica was exposed under the same conditions as those used for studying oxidation reactions (total flow, complete darkness) but without any oxidant. As no loss of BaP was observed under these experimental conditions, desorption of BaP was considered as negligible and degradation of BaP was fully attributed to the only reactions with the different oxidants.

3.3 Reactions of BaP with ozone

All experimental data for this reaction were plotted on a same single graph, presented in Figure 1, for a reference ozone concentration of $[\text{O}_3]_{\text{ref}} = 1.4 \times 10^{13} \text{ molecule cm}^{-3}$. Initial BaP concentration was $(353 \pm 65) \mu\text{g g}^{-1}$ ($n = 24$).

Reaction of ozone with BaP adsorbed on silica particles was almost complete after 3 min under our experimental conditions. 12 replicates for each reaction time were available for the fit to derive the pseudo-first order rate constant (k^{I}). The kinetics of BaP degradation was also investigated as a function of O_3 concentration. In Figure 2 are presented pseudo-first order rate constant values as a function of O_3 concentration fitted by a straight line. This Figure allows to verify that the reactivity of BaP was proportional to the oxidant concentration under

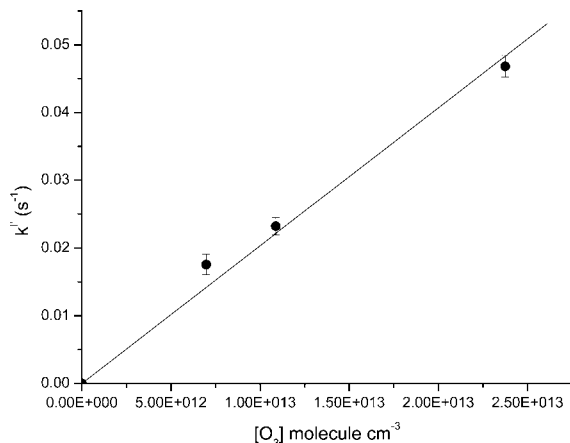


Fig. 2. Pseudo-first order rate constants for the reaction of silica-bound-BaP with ozone as a function of ozone concentration and corresponding linear regressions. Error bars represent 2 standard deviations on the exponential coefficient obtained from the non-linear least square fitting of experimental points.

our experimental conditions, demonstrating the elementary nature of the reaction. According to line slopes, second order rate constants were determined for the reactions of O₃ to be $(2.1 \pm 0.5) \times 10^{-15} \text{ cm}^3 \text{ molecule}^{-1} \text{ s}^{-1}$, at room temperature.

The first order dependence of the BaP decay observed in this study was already reported for other PAH or for different particulate support [5, 51, 57, 66]. On the contrary, Pöschl *et al.* [59] and Kwamena *et al.* [39, 40] observed a Langmuir-Hinshelwood behaviour and considered a reaction mechanism where ozone is first adsorbed to the surface prior to reacting with BaP. They specified that there is a maximum for pseudo-first order constant values when all active sites of the support are saturated by oxidant molecules. Observation of this mechanism was made for laboratory-soot particles [59] and for azelaic acid aerosols [39, 40]. Up to now, no Langmuir-Hinshelwood behaviour was observed for silica gel [5] and silica plates [66], experiments being all performed in the same range of ozone concentration (2.5×10^{12} to $8 \times 10^{14} \text{ molecule cm}^{-3}$). This question is therefore still under consideration.

Another parameter largely influencing the heterogeneous reactivity of BaP is the particle loading. A previous study by our group [57] of the reactivity of BaP adsorbed on silica but in a mixture with 12 other PAH-congeners (with similar particulate concentrations) and exposed to ozone led to a second order rate constant of $(1.4 \pm 0.3) \times 10^{-16} \text{ cm}^3 \text{ molecule}^{-1} \text{ s}^{-1}$ at room temperature. Experiments were performed using the same silica particles, the same particulate-BaP loading and the same experimental set-up. Even accounting for the presence of other PAHs on the silica to react with ozone (their reactivity being measured

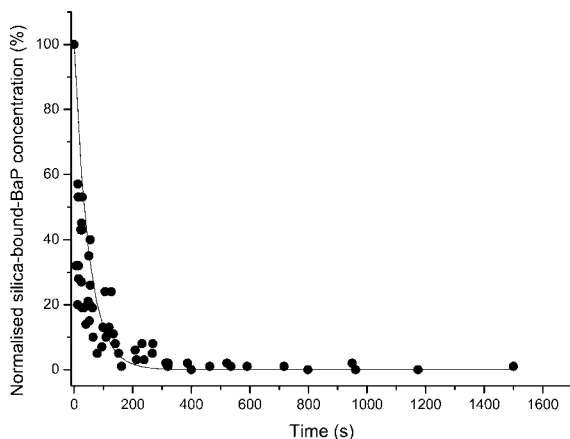


Fig. 3. Normalised concentration of BaP adsorbed on silica particles as a function of NO_2 exposure time, represented for $[\text{NO}_2] = 3.5 \times 10^{13} \text{ molecule cm}^{-3}$.

simultaneously) and therefore decreasing the amount of ozone available to only react with BaP, this does not allow to explain the factor of 15 existing between the rate constant value previously reported by Perraudin et al. [57] and that measured in this work. It is clear that the nature (specific surface area, composition,...) of the coating particle strongly influences heterogeneous reaction mechanisms and therefore the rate of BaP degradation. The influence of the close environment of the PAH on the particle was already reported and discussed [5, 10, 17, 18] but is still difficult to interpret as the total amount of PAH in almost all reported works (including this one) corresponds to a total surface coverage less than 10% of a monomolecular layer. The influence of the BaP particle loading will be carefully carried out in a future study, focusing particularly on the possible presence of PAH aggregates and on the different adsorption sites to be considered on the silica surface.

3.4 Reactions of BaP with NO_2

A similar procedure was applied for the reaction of nitrogen dioxide with BaP adsorbed on silica particles. BaP concentration decay when reacting with NO_2 is presented in Figure 3, for a reference nitrogen dioxide concentration of $3.5 \times 10^{13} \text{ molecule cm}^{-3}$. Initial BaP concentration was $(479 \pm 31) \mu\text{g g}^{-1}$ ($n = 21$). Reaction of nitrogen dioxide with BaP adsorbed on silica particles was observed to be complete after 3–4 min. Influence of nitrogen dioxide concentration was also investigated using three different concentrations and the elementary nature of the reaction was again demonstrated. Results are presented in Figure 4. According to line slopes, second order rate constant was determined for the reaction to be $(5.8 \pm 1.4) \times 10^{-16} \text{ cm}^3 \text{ molecule}^{-1} \text{ s}^{-1}$, at room temperature.

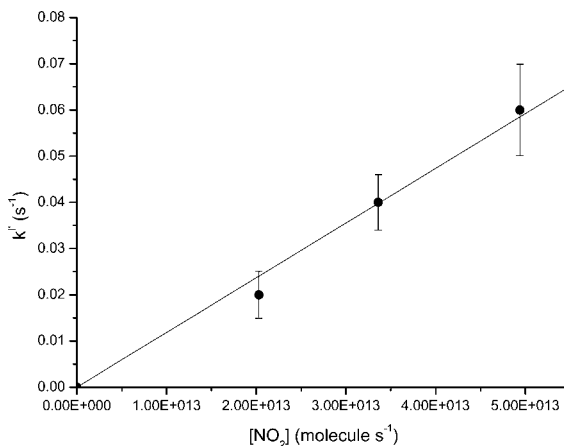


Fig. 4. Pseudo-first order rate constants for the reaction of silica-bound-BaP with nitrogen dioxide as a function of NO₂ concentration and corresponding linear regression. Error bars represent 2 standard deviations on the exponential coefficient obtained from the non-linear least square fit of experimental points.

As observed above for ozone, our group also previously reported a different (1.6 times higher) rate constant for the NO₂ reaction [56]. Again, BaP was adsorbed in that work on particles of different types among a mixture of twelve other PAHs. Such a difference is still not very clear or easy to explain, despite the very large number of experiments in both works and the very good reproducibility and repeatability of the results. Note that Miet *et al.* [51] also recently showed that the reactivity of pyrene (a 4-rings PAH) is 4 times larger when adsorbed alone on particles (as a model) than when being present in a complex mixture.

Different uptake studies previously made on thin films of PAHs did not show any reaction when exposed to NO₂ but the same reaction appears efficient with PAHs adsorbed on n-hexane soot [24, 39]. The amount of PAHs adsorbed on partially or completely covered particle surface, strongly influences the reaction rates. As explained above in the ozone reaction section, considering a high PAH concentration and according to the specific surface area of the particle, PAH may form aggregates and become less accessible to the oxidants. On the contrary, PAHs with low coating concentration are mono-dispersed on the surface and will more accessible to the oxidant, as previously suggested by Kamens *et al.* [31]

3.5 Reactions of BaP with OH

A decay of particle-bound BaP concentration versus hydroxyl radical (in the presence of NO₂) exposure time is presented in Figure 5. Initial BaP concentration was (476±62) μg g⁻¹ (n = 15). The reaction was complete after 1.5 min. Since it was not possible to accurately calibrate OH concentration in this work

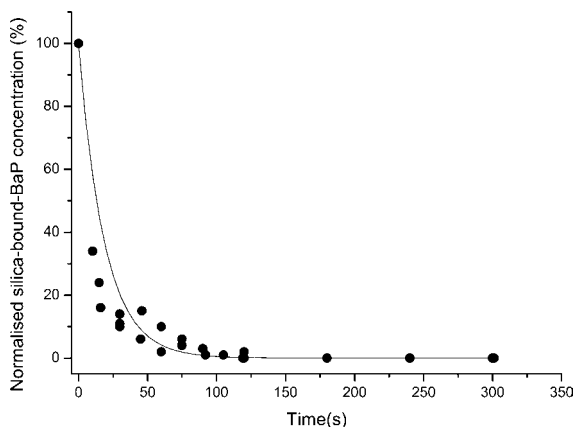


Fig. 5. Decay of normalised concentration of silica-bound BaP vs. exposure time to hydroxyl radicals in the presence of nitrogen dioxide.

and therefore propose a second order rate constant for this reaction, only a pseudo-first order rate constant was derived from the fit, leading $k_{(\text{BaP} + \text{OH})}^{\text{I}} = (3.4 \pm 0.8) \times 10^{-2} \text{ s}^{-1}$. Such a value was obtained after the subtraction of the NO_2 contribution to the total BaP decay.

Note that the only estimation of the OH initial concentration proposed in this work allows us to conclude that the heterogeneous reaction of OH with BaP ($k_{(\text{BaP} + \text{OH})}^{\text{II}} \approx 5.9 \times 10^{-14} \text{ cm}^3 \text{ molecule}^{-1} \text{ s}^{-1}$) is much faster than those of ozone and NO_2 but slower than the usual corresponding reaction of OH with (lighter) PAHs occurring in the gas phase, meaning that heterogeneous processes of BaP with OH are negligible under atmospheric conditions (considering an averaged atmospheric OH concentration of $\approx 1 \times 10^6 \text{ molecule cm}^{-3}$).

3.6 Oxidation products

In this work, degradation products were investigated by GC-MS only for the reactions of silica-bound BaP with NO_2 and OH. Reaction products arising from ozone initiated oxidation of BaP will be presented in another article.

3.6.1 Reaction with nitrogen dioxide

In order to identify the largest number of products, mass detection was first performed in the scan mode (mass/charge ratio ranging from 50 to 550). Pulsed splitless mode injection (purge flow = $1 \text{ cm}^3 \text{ s}^{-1}$, purge time = 60 s, 25 psi pulse during 60 s) was added to the previous chromatographic parameters in order to enhance the analyte transfer in the head of the analytical capillary column.

The chromatograms presented only three new peaks after the reaction of BaP with NO_2 (Figure 6). A comparison of the corresponding mass spectra with

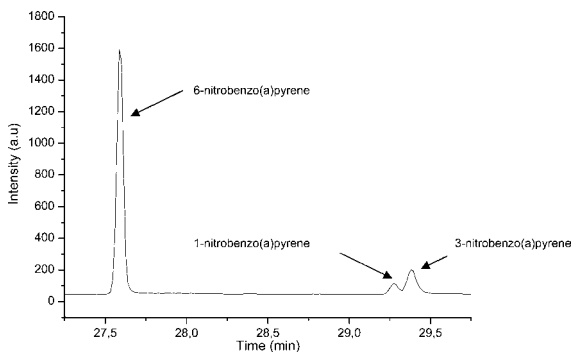


Fig. 6. Chromatogram of products from the reaction of silica-bound BaP with nitrogen dioxide.

those reported in the mass spectra library (NIST 98, HP Mass Spectral Library, 1998) allowed the identification of these compounds as three nitrobenzo(a)pyrenes (NBaP). 6-nitrobenzo(a)pyrene was identified by its retention time injecting a standard solution. 1- and 3-nitrobenzo(a)pyrenes were only identified by comparison with chromatograms already reported in the literature [30, 38]. Note that at longer exposure times than those allowing the total degradation of BaP, it was observed the further formation of dinitrobenzo(a)pyrenes (diNBaP), parallelly to the decrease of the concentrations of 1-, 3- and 6-nitrobenzo(a)pyrenes. At least two compounds are expected to be formed by this way: 1,6- and 3,6-dinitrobenzo(a)pyrenes. Unfortunately, their identification was not made possible in this work.

Ishii *et al.* [30] have previously shown the formation of all these compounds studying the reaction of BaP-coated glass fiber filter exposed to 10 ppm of nitrogen dioxide. They estimated that 70 % of total initial BaP concentration were converted in mononitroBaP. It was also shown in that work that amounts of dinitroBaP increased gradually and then decreased slowly.

In the present study, GC-MS single ion monitoring mode was applied for the product quantification. NBaP were quantified by external calibration: three solutions of 6-nitrobenzo(a)pyrene were prepared with quantities ranging from 0.74 to 9.19 ng injected on the column. These solutions were injected before, between and after each analysis. The major product for the NO_2 reaction was the 6-NBaP isomer with smaller yields of the 1- and 3- isomers. Experimental data shows that 6-NBaP accounts for (83 ± 6) % of all nitrated BaP formed, 1-NBaP for (5 ± 2) % and 3-NBaP for (12 ± 5) % ($n = 25$). The distribution of isomeric mononitro-BaP derivatives generally followed the electron densities calculated for various positions in the molecule. Carbon balance for investigated reaction was therefore complete within uncertainties, confirming that the oxidation products identified in this study are the only products formed in the system. Note that these results are in very good agreement with those reported previously by Ishii *et al.* [30].

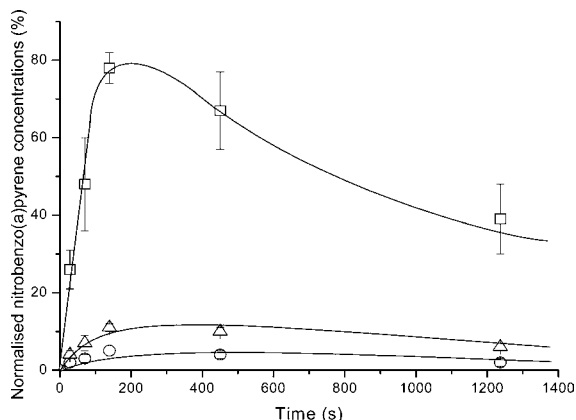


Fig. 7. Normalised concentrations of 6-(square), 1-(circle) and 3-(triangle)NBaP for different exposure time to nitrogen dioxide (with $[\text{NO}_2] = 3.5 \times 10^{13} \text{ molecule cm}^{-3}$). Error bars represent 2 standard deviations corresponding to the statistical uncertainty evaluated from 5 experimental replicates.

The product quantification also allowed us to determine the product formation rates. Indeed, normalised product concentrations within NO_2 exposure time were fitted using first order exponential functions (Figure 7). Note that it was logically assumed that nitro- and dinitroBaP were not desorbing along the reaction time, as they present lower vapor pressures than BaP. Second order rate constant values for product formations were determined to be $3.7 \times 10^{-16} \text{ cm}^3 \text{ molecule}^{-1} \text{ s}^{-1}$ for 6-NBaP, $2.2 \times 10^{-17} \text{ cm}^3 \text{ molecule}^{-1} \text{ s}^{-1}$ for 1-NBaP and $5.3 \times 10^{-17} \text{ cm}^3 \text{ molecule}^{-1} \text{ s}^{-1}$ for 3-NBaP, leading to a global value of $4.45 \times 10^{-16} \text{ cm}^3 \text{ molecule}^{-1} \text{ s}^{-1}$ for all mononitrated BaP formation. This value is still reasonable considering all the uncertainties on the four different compounds to be considered. After 3–4 min of reaction, NBaP concentrations start to decrease and a small amount of diNBaP was detected. Second order rate constants derived for the NO_2 degradation of NBaP were estimated to be $1.8 \times 10^{-17} \text{ cm}^3 \text{ molecule}^{-1} \text{ s}^{-1}$ for 6-NBaP, $2.2 \times 10^{-17} \text{ cm}^3 \text{ molecule}^{-1} \text{ s}^{-1}$ for 1-NBaP and $1.9 \times 10^{-17} \text{ cm}^3 \text{ molecule}^{-1} \text{ s}^{-1}$ for 3-NBaP, all these values being considered to be similar within uncertainties.

A possible mechanism explaining the formation of the three NBaP could be the first addition of NO_2 to the most electrophilic carbon atoms (positions 6, 3 and 1 for benzo(a)pyrene [58]), followed by a second addition of NO_2 in the alpha position to finally lead to a elimination of HONO occurring by the abstraction of a hydrogen atom from the first carbon (Figure 8). Such a mechanism has

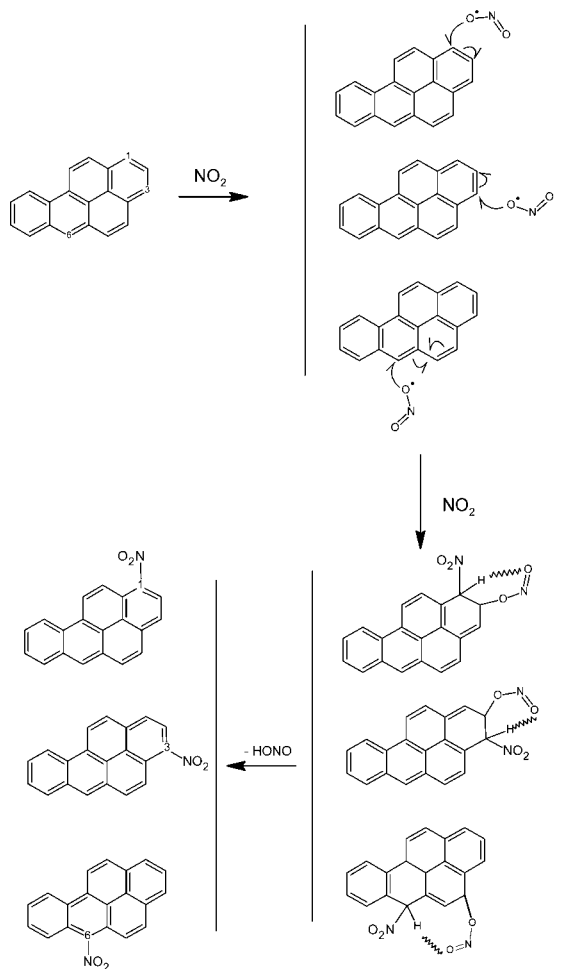


Fig. 8. Mechanism proposed for the heterogeneous nitration of benzo(a)pyrene.

already been recently proposed by our group in the similar case of pyrene reaction [51].

3.6.2 Reaction with hydroxyl radical

Product identification was also performed by GC-MS in the scan mode using the same chromatographic parameters as described above.

Due to the method of OH production in the reactor (a large excess of NO_2 reacting with H atoms), nitrogen dioxide was the major reactive species in the reaction system. Therefore, all the three nitrated-BaP were again identified and quantified. But this time, the total yield of degraded BaP was estimated to be

not more than 20–25 %. As in the case of the reaction with nitrogen dioxide only, 6-NBaP relatively accounted for approximately 80 % of total nitrated species formed, 1-NBaP for 5% and 3-NBaP for 15 %. Consequently, it is likely that the nitro-BaP formation was following the same mechanism under our experimental condition. Another mechanism for the formation of nitrated compounds has been reported for the PAH in the gas phase in the presence of nitrogen dioxide [9, 61]. It first involves the addition of OH, then NO₂ is adding in the alpha position to finally lead to a departure of H₂O occurring by the abstraction of a hydrogen atom from position 1.

In this work, derivation of samples with BSTFA (bis(trimethylsilyl)-trifluoroacetamide) (25 μl, 30 min at 65°C) allowed to also detect hydroxylated compounds. Samples were injected before and after derivation. Monohydroxylated ($m/z = 268$) and a small amount of three different dihydroxylated ($m/z = 284$) compounds were detected. Unfortunately, comparison of the mass spectra obtained with those reported from the NIST mass spectra library did not clearly allow us to better identify these compounds.

4. Conclusions

In this work, rate constants were measured for the reactions of O₃, NO₂ and OH with benzo(a)pyrene adsorbed on silica particles, in the darkness and at room temperature. Second order rate constants were measured to be $(2.1 \pm 0.5) \times 10^{-15} \text{ cm}^3 \text{ molecule}^{-1} \text{ s}^{-1}$ for the reaction with O₃ and $(5.8 \pm 1.4) \times 10^{-16} \text{ cm}^3 \text{ molecule}^{-1} \text{ s}^{-1}$ for the reaction with NO₂. Only pseudo-first order rate constant could be obtained for the reaction of BaP with OH: $k^1 = (3.4 \pm 0.8) \times 10^{-2} \text{ s}^{-1}$. Degradation products were investigated in the case of the reactions with NO₂ and OH. 1-, 3- and 6-nitrobenzo(a)pyrenes were found to be the major oxidation products from the (BaP + NO₂) reaction. The global kinetics of product formation has been demonstrated to be similar to that measured for the BaP degradation, within uncertainties. Dinitrobenzo(a)pyrenes were also identified when no more BaP was detected but it was not possible for them to be quantified. Results obtained for nitro-BaP are in very good agreement with those previously obtained by Ishii et al. [30]. Product identification was also performed for the reaction of BaP with OH in the presence of a large excess of NO₂. 1-, 3-, and 6-nitroBaP were again detected and it appears that their formation was following the same mechanism for both NO₂ and OH (in the presence of NO₂) reactions under our experimental conditions, but with a lower efficiency. Mono- and di-hydroxylated compounds were also detected but not identified in this work.

Further work will be necessary to better calibrate the initial OH concentration in our experiments, to allow to propose second order rate constants useful to extrapolate atmospheric lifetimes but also to give rise to evaluate the formation of HONO and/or H₂O.

Heterogeneous mechanisms involved for all reactions were not clearly understood in this work but again Langmuir-Hinshelwood mechanism could not be clearly retained from the observations described in this study. Such mechanisms are often debated and it is clear that the particulate substrate is one of the most important parameter. Particle loading and adsorption state of adsorbed-PAHs (mono-dispersed, aggregates, amorphous or crystalline) are essential parameters to focus on in the next future to better understand heterogeneous reactivity.

Finally, the nitrated products identified in this work are very important, as being recognized to be very toxic and particularly mutagenic [30, 46, 47]. Identification of all other BaP oxidation products will be carried on performing new analytical developments as it is of major importance to improve the evaluation of their impact on human health.

Acknowledgement

The authors wish to thank the French National Research Agency and the Aquitaine Region for financial support.

References

1. C. Adelhelm, R. Niessner, U. Pöschl, T. Letzel, *Analytical and Bioanalytical Chemistry* **391** (2008) 2599.
2. Albinet, E. Leoz-Garziandia, H. Budzinski, E. Villenave, *Sci. Total Environ* **384** (2007) 280.
3. Albinet, E. Leoz-Garziandia, H. Budzinski, E. Villenave, J. L. Jaffrezo, *Atmos. Environ* **42** (2008a) 55.
4. Albinet, E. Leoz-Garziandia, H. Budzinski, E. Villenave, J. L. Jaffrezo, *Atmos. Environ* **42** (2008b) 43.
5. Alebic-Juretic, T. Cvitas, L. Klasinc, *Environ Sci. Technol.* **24** (1990) 62.
6. Alebic-Juretic, T. Cvitas, L. Klasinc, *Chemosphere* **41** (2000) 667.
7. J. O. Allen, N. M. Dookeran, K. Taghizadeh, A. L. Lafleur, K. A. Smith, A. F. Sarofim, *Environ. Sci. Technol.* **31** (1997) 2064.
8. M. Ammann, M. Kalberer, D. T. Jost, L. Tobler, E. Rössler, D. Piguet, H. W. Gäggeler, U. Baltensperger, *Nature* **395** (1998) 157.
9. R. Atkinson, J. Arey, B. Zielinska, S. M. Aschmann, *Environ. Sci. Technol.* **21** (1987) 1014.
10. T. D. Behymer, R. A. Hites, *Environ. Sci. Technol.* **19** (1985) 1004.
11. A. K. Bertram, A. V. Ivanov, M. Hunter, L. T. Molina, M. J. Molina, *J. Phys. Chem. A.* **105** (2001) 9415.
12. G. L. Borosky, K. K. Laali, *Organic and Biomolecular Chemistry* **5** (2007) 2234.
13. W. F. Busby Jr, H. Smith, C. L. Crespi, B. W. Penman, *Mutation Research - Genetic Toxicology* **342** (1995) 9.
14. M. A. A. Clyne, P. B. Monkhouse, *Journal of the Chemical Society, Faraday Transactions 2: Molecular and Chemical Physics* **73** (1977) 298.
15. W. Estève, *Thèse de Doctorat de l'Université de Bordeaux* **1** (2002).
16. W. Estève, H. Budzinski, E. Villenave, *Polycyclic Aromatic Compounds* **23** (2003) 441.
17. W. Estève, H. Budzinski, E. Villenave, *Atmos. Environ* **38** (2004) 6063.
18. W. Estève, H. Budzinski, E. Villenave, *Atmos. Environ* **40** (2006) 201.

19. B. J. Finlayson-Pitts, P. J. N. Jr., *Atmospheric chemistry, Fundamentals and experimental techniques*. Wiley Interscience Editions, New York (1986).
20. B. J. Finlayson-Pitts, J. N. Pitts Jr., *Science* **276** (1997) 1045.
21. B. J. Finlayson-Pitts, L. M. Wingen, A. L. Sumner, D. Syomin, K. A. Ramazan, *Physical Chemistry Chemical Physics* **5** (2003) 223.
22. A. L. Goodman, G. M. Underwood, V. H. Grassian, *J. Phys. Chem. A.* **103** (1999) 7217.
23. V. H. Grassian, *J. Phys. Chem. A.* **106** (2002) 860.
24. S. Gross, A. K. Bertram, *J. Phys. Chem. A.* **112** (2008) 3104.
25. A. I. Guilloteau, M. L. Nguyen, Y. Bedjanian, G. Le Bras, *J. Phys. Chem. A.* **112** (2008) 10552.
26. M. K. D. Hailwood, E. Leotz-Garzianda, R. Maynard, E. Menichi, S. Moorcroft, J. Pacyna, P. Perez Ballesta, J. Schneider, R. Westerholm, M. Wichmann-Fiebig, M. Woodfield, L. Van Bree, C. Conolly, Office for Official Publications of the European Communities (2001).
27. K. Horikawa, N. Sera, K. Murakami, N. Sano, K. Izumi, H. Tokiwa, *Toxicology Letters* **98** (1998) 51.
28. IARC. (2008). "Complete List of Agents evaluated and their classification: Agents reviewed by the IARC monographs."
29. Retrieved <http://monographs.iarc.fr/ENG/Classification/Listagentsalphorder.pdf> consulted in February 2009.
30. S. Ishii, Y. Hisamatsu, K. Inazu, T. Kobayashi, K. I. Aika, *Chemosphere* **41** (2000) 1809.
31. R. M. Kamens, *Environ. Sci. Technol.* **22** (1988) 103.
32. R. M. Kamens, J. M. Perry, D. A. Saucy, *Env. Int.* **11** (1985) 131.
33. L. H. Keith, W. A. Telliard, *Environ. Sci. Technol.* **13** (1979) 416.
34. U. Kirchner, V. Scheer, R. Vogt, *J. Phys. Chem. A.* **104** (2000) 8908.
35. J. Kleffmann, P. Wiesen, *Atm. Chem. Phys.* **5** (2005) 77.
36. R. Koeber, J. M. Bayona, R. Niessner, *Environ. Sci. Technol.* **33** (1999) 1552.
37. R. Koeber, R. Niessner, *J. Aerosol Sci.* **28** (1997).
38. R. L. Kristovich, P. K. Dutta, *Environ. Sci. Technol.* **39** (2005) 6971.
39. N. O. A. Kwamena, J. P. D. Abbatt, *Atmos. Environ.* **42** (2008) 8309.
40. N. O. A. Kwamena, M. G. Staikova, D. J. Donaldson, I. J. George, J. P. D. Abbatt, *J. Phys. Chem. A.* **111** (2007) 11050.
41. N. O. A. Kwamena, J. A. Thornton, J. P. D. Abbatt, *J. Phys. Chem. A.* **108** (2004) 11626.
42. S. Lelievre, Y. Bedjanian, N. Pouvesle, J. L. Delfau, C. Vovelle, G. Le Bras, *Physical Chemistry Chemical Physics* **6** (2004) 1181.
43. M. Letellier. Thèse de Doctorat de l'Université de Bordeaux 1 (1998).
44. T. Letzel, E. Rosenberg, U. Pöschl, R. Niessner, *J. Aerosol Sci.* **30** (1999) S605.
45. L. Ley. Thèse de Doctorat de l'Université de Bordeaux 1 (1995).
46. V. Librando, A. Alparone, *J. Hazard, Mater.* **161** (2009) 1338.
47. V. Librando, A. Alparone, G. Tomaselli, *J. Mol. Mod.* **14** (2008) 489.
48. J. C. Loison, L. Ley, R. Lesclaux, *Chem. Phys. Lett.* **296** (1998) 350.
49. Messerer, R. Niessner, U. Pöschl, *Carbon* **44** (2006) 307.
50. K. Miet. Thèse de Doctorat de l'Université de Bordeaux 1 (2008).
51. K. Miet, K. Le Menach, P. M. Flaud, H. Budzinski, E. Villenave, *Atmos. Environ.* **43** (2009) 837.
52. Naspinski, R. Lingenfelter, L. Cizmas, Z. Naufal, L. Y. He, A. Islamzadeh, Z. Li, Z. Li, T. McDonald, K. C. Donnelly, *Env. Int.* **34** (2008) 988.
53. M. L. Nguyen. Thèse de Doctorat de l'Université d'Orléans (2008).
54. Papastefanou, *Appl. Radiat. Isot.* **64** (2006) 93.
55. Perraudin, H. Budzinski, E. Villenave, *Analytical and Bioanalytical Chemistry* **383** (2005a) 122.

56. Perraudin, H. Budzinski, E. Villenave, *Atmos. Environ.* **39** (2005b) 6557.
57. Perraudin, H. Budzinski, E. Villenave, *J. Atm. Chem.* **56** (2007) 57.
58. J. N. Pitts Jr., *Environmental Health Perspectives* **47** (1983) 115.
59. U. Pöschl, T. Letzel, C. Schauer, R. Niessner, *J. Phys. Chem. A.* **105** (2001) 4029.
60. M. S. Salgado, M. J. Rossi, *Int. J. Chem. Kinet.* **34** (2002) 620.
61. J. Sasaki, S. M. Aschmann, E. S. C. Kwok, R. Atkinson, J. Arey, *Environ. Sci. Technol.* **31** (1997) 3173.
62. US-EPA. EPA 540/1-86-013 Cincinnati OH:Environmental Criteria and Assessment Office (1984).
63. C. R. Usher, A. E. Michel, V. H. Grassian, *Chemical Reviews.* **103** (2003) 4883.
64. G. M. Underwood, P. Li, H. Al-Abadleh, V. H. Grassian, *J. Phys. Chem. A.* **105** (2001) 6609.
65. K. A. Van Cauwenberghe, L. Van Vaeck, J. N. J. Pitts, *Forensic Environmental Applications.* (1984) 1499.
66. C. H. Wu, I. Salmeen, H. Niki. *Environ. Sci. Technol.* **18** (1984) 603.